

# Intermediate Structures for Higher Level Arrangements: Catching Disk-Like Micelles in Decane Phosphonic Acid Aqueous Solutions

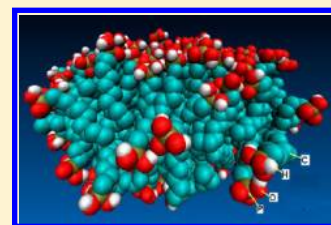
Erica P. Schulz,<sup>†</sup> Ángel Piñero,<sup>‡</sup> José L. Rodríguez,<sup>†</sup> Rosana M. Minardi,<sup>†</sup> Marisa Frechero,<sup>†</sup> and Pablo C. Schulz<sup>\*,†</sup>

<sup>†</sup>Departamento de Química e Instituto de Química del Sur (INQUISUR-CONICET), Universidad Nacional del Sur, Bahía Blanca, Argentina

<sup>‡</sup>Soft Matter & Molecular Biophysics Group, Department of Applied Physics, University of Santiago de Compostela, CP 15872 Santiago de Compostela, Spain

## Supporting Information

**ABSTRACT:** It has been proposed that disk-like micelles may be precursors to the formation of lamellar liquid crystals. The possibility of obtaining *n*-decane phosphonic acid (DPA) disk-like micelles in aqueous solution without the addition of a second ionic surfactant led us to study in detail the low-concentration range of this system by both a battery of experimental techniques and molecular dynamics (MD) simulations. The experimental results indicate that premicelles with some capacity to solubilize dyes are formed at 0.05 mM. The critical micelle concentration (cmc) was found to be  $0.260 \pm 0.023$  mM, much lower than that previously reported in the literature. Spherical micelles, which immediately grow, leading to disk-like micelles, are probably formed at this concentration. At  $0.454 \pm 0.066$  mM, disk-like micelles become unstable, giving rise to the formation of an emulsion of lamellar mesophase that dominates the system beyond  $0.670 \pm 0.045$  mM. These experimental results were corroborated by MD simulations which, additionally, allow describing the structure of the obtained micelles at atomic level. The analysis of the MD trajectories revealed the presence of strong intermolecular hydrogen bonds between the surfactant headgroups, producing a compact polar layer with low water content. The formation of such H-bond network could explain the ability of this surfactant to form disk-like micelles at concentrations close to the cmc.



## INTRODUCTION

While spherical and rod-like micelles are commonly found in surfactant systems, disk-like micelles are rather seldomly reported. This could be explained by the difficulty to stabilize such structures due to their perimeter line tension. Thus, aggregates often grow, giving rise to the formation of large bilayers which may fold to form vesicles.<sup>1</sup> Disk-like micelles (also named bicelles) can be formed as an intermediate structure by a technique named “detergent depletion” which uses mixed micelles of uncharged phospholipids and conventional surfactants.<sup>2–5</sup> These intermediate structures are transformed into vesicles by removing the conventional surfactant. Disk-like micelles can be stabilized by the accumulation of the conventional surfactant in the edges of the micelle. The elimination of these molecules causes destabilization by exposition of the hydrophobic side of the micelle to water. This, in turn, provokes the growth of the disk-like micelles which become large bilayers and subsequently seal off their exposed hydrophobic edges to form vesicles. A generalization of this model postulates that disk-like micelles can be formed in some cases without the presence of another amphiphile, as short-lived “flakes” or fragments of bilayers.<sup>6</sup> Such structures form vesicles upon sonication or when they are forced to pass through narrow filters. Transition structures are difficult to study due to their instability and small existence domains.<sup>6</sup>

Disk-like micelles of phospholipids have been predicted from energetic considerations as intermediates in the vesicle pathway

formation.<sup>7–9</sup> This process was described in the literature for bile salt/lecithin mixtures.<sup>10</sup> When uncharged phospholipids are exposed to water, tubular structures called myelin figures grow, often forming vesicles. DPA was proved to spontaneously form vesicles in aqueous solution.<sup>11,12</sup> Large thermodynamically stable disk-like micelles composed of a drug and a biological lipid have been reported as novel drug delivery systems.<sup>13</sup> Since vesicles consist of lamellar liquid crystals, the existence of disk-like micelles close to the lamellar mesophase existence domain is feasible.

Alcanephosphonic acid crystals exposed to water have also proved to form vesicles, and they could follow the same pathway, having disk-like micelles as intermediate structures.

Decanephosphonic acid ( $C_{10}H_{21}PO_3H_2$ , DPA) forms anhydrous crystals which in contact with water produce lamellar liquid crystals.<sup>11</sup> The cmc reported in the literature for this compound between 20 and 80 °C is 1.66 mM.<sup>14</sup> Since vesicles are formed by lamellar liquid crystals, the existence of disk-like micelles close to the lamellar mesophase domain is a feasible possibility. The possibility of obtaining bicelles without addition of a second ionic surfactant with DPA aqueous solutions led us to study in detail the low-concentration range of this system by both a battery of experimental techniques and molecular

**Received:** December 24, 2012

**Revised:** April 29, 2013

dynamics simulations. This allows us to obtain detailed information of the studied system in a large range of time and size scales.

Using the excluded area per phosphonic acid headgroup obtained from the polar headgroup partial molar volume in micellized state ( $a = 0.35 \pm 0.13 \text{ nm}^2$ ),<sup>15</sup> as well as the length and volume of the hydrocarbon chain using data from refs 16 and 17, respectively ( $l = 1.4704 \text{ nm}$ ;  $v = 0.5162 \text{ nm}^3$ ), the packing parameter was found to be  $P = v/al = 1.00$ . As stated by Israelachvili, Mitchell, and Ninham,<sup>18</sup> this value indicates the formation of lamellar structures. On the basis of these geometrical considerations, the possibility of bicelle formation at very low concentrations was investigated.

## EXPERIMENTAL SECTION

Decanephosphonic acid was synthesized and characterized as described elsewhere. The surfactant was recrystallized three times using petroleum ether fraction 60–80 °C and purity was controlled with FT-IR, <sup>1</sup>H NMR, melting point, and elemental analysis, giving a purity of 99.6%.<sup>19</sup> A 15.78 mM DPA aqueous solution was prepared and employed to perform the experiments. Conductivity measurements were made with an automatic Instrumentalia Antares II conductimeter. The instrument was calibrated with KCl aqueous solutions, as usual. The pH determinations were made with a CRIBABB millivoltmeter and pH-meter using a Broade and James glass electrode. Absorbance measurements at  $\lambda = 450 \text{ nm}$  were performed with a Spectronic 20 UV–vis spectrophotometer by titration of the concentrated solution on water. Dye solubilization experiments were made by addition of Sudan III crystals to DPA solutions as a function of the surfactant concentration. After resting for a week with periodical agitation, the supernatant absorbance was measured at  $\lambda = 488 \text{ nm}$  using the same instrument. Optical microscopy was performed with a Nikon Eclipse E-200 POL polarizing microscope. Crystals of DPA were placed between slides, and a droplet of water was introduced in one side of the sample following the peripheral dilution method. The resulting textures were recorded with a digital camera. A digital vibro viscosimeter Cole-Parmer SV-10 calibrated with water was employed to measure the viscosity of the solutions with  $\pm 1\%$  repeatability.

**Molecular Dynamics Simulations.** MD simulation studies at five different surfactant concentrations were performed to investigate the formation of self-assembled structures along the trajectories. The systems were built by placing 40, 60, 90, 120, and 150 DPA molecules at random positions and orientations in cubic boxes which were then filled with about 10 000 preequilibrated water molecules. The surfactant molecules were modeled by using the G53a6<sup>20</sup> parametrization of the GROMOS96 force field with the bonded parameters and partial charges taken from Roy et al.<sup>21</sup> Results obtained from the Automated Topology Builder (ATB)<sup>22</sup> for DPA were also taken as a reference. The simple point charge (SPC) water model was utilized to simulate the solvent in an explicit way. An energy minimization using the steepest descent method was performed for all of the systems. Three-dimensional periodic boundary conditions with cubic boxes were used for all of the trajectories. For the production simulations, water and surfactant molecules were separately coupled to a  $v$ -rescale thermostat with a common period of 0.1 ps. The pressure was isotropically controlled by using a Parinello–Rahman barostat with a coupling constant of 0.5 ps and considering an isothermal compressibility of  $4.5 \times 10^{-5} \text{ bar}^{-1}$ . Long range

electrostatic interactions were calculated using the particle mesh Ewald method with a real-space cutoff of 1.2 nm, a 0.15 spaced grid, and a fourth order B-spline interpolation. Random initial velocities were assigned to the systems from a Maxwell–Boltzmann distribution at 298 K. The equations of motion were integrated using the leapfrog method with a time step of 2 fs. Bond lengths and angles in water were constrained using the SETTLE algorithm, while the LINCS algorithm was used to constrain bond lengths within the surfactant molecules. Using these parameters, a 100 ns long trajectory at 298 K and 1 bar was performed for each of the five systems using the GROMACS package,<sup>23–25</sup> version 4.5.1. The analysis of the trajectories was performed using tools of the GROMACS package, as well as programs specifically developed for this work.

## RESULTS

**Experimental Section.** The 15.78 mM DPA solution, about 10 times the cmc value reported in the literature for this compound, looks like a white emulsion. This system observed in a polarizing microscope shows a suspension of nearly spherical particles and irregular aggregates of them (Figure 1).

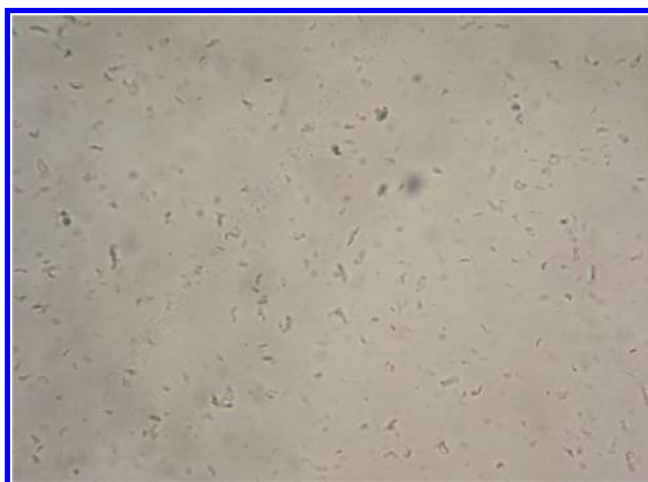


**Figure 1.** Photomicrograph of the 15.78 mM DPA suspension in water, X400.

Depending on the size and orientation, some of the particles show birefringence (Figure 1 in the Supporting Information). Upon dilution to half the cmc value reported in the literature, the solution still looks like a suspension. The texture of the birefringent particles is not clear, but since in the peripheral dilution of crystals with water myelin figures, vesicles and spherulites are formed (see Figure 2), it was concluded that the suspension is formed by lamellar liquid crystalline particles. The fact that some particles do not show birefringence is due to the isotropicity of the system, as observed from perpendicular views to the lamellae planes of the mesophase. No sedimentation was observed upon 20 min of centrifugation at  $3000 \text{ min}^{-1}$ .

Figure 3 shows the absorbance of DPA aqueous solutions at  $\lambda = 450 \text{ nm}$  as a function of the surfactant concentration. Large particles are observed up to about 0.2 mM. Two transitions appear at 0.44 and 1.1 mM.

The absorbance of Sudan III solubilized in DPA solutions shows three transitions at 0.05, 0.25, and 0.52 mM (Figure 4). These transitions are expected to be related to the formation of spherical, rod-like, and/or disk-like micelles, respectively. The

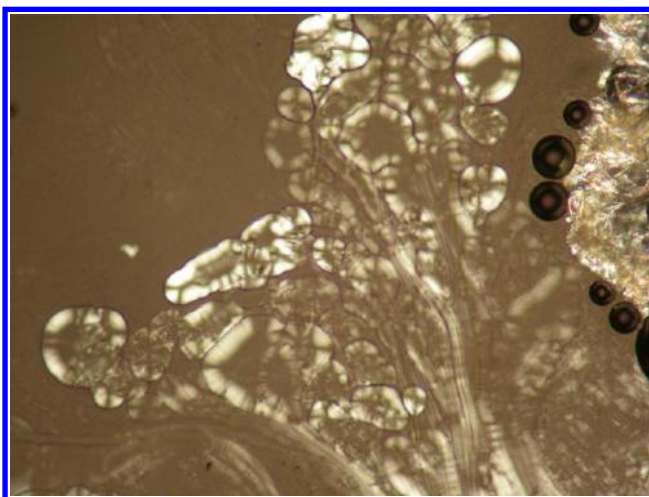


**Figure 2.** Photomicrograph of the peripheral dilution of DPA crystals in water. Right: crystals. Center: myelin figures, vesicles, and negative spherulites. Left: isotropic solution. Crossed polarizers, X100.

larger Laplace pressure of spherical micelles when compared to rod-like and disk-like micelles makes the dye less soluble in the former, which explains the slope increase between 0.25 and 0.52 mM. On the other hand, the very low solubilization of the dye below 0.05 mM may be caused by the presence of small pre-micelles.<sup>26</sup> Above 0.52 mM, many DPA molecules may be unable to solubilize the dye because much of the surfactant is inside the mesophase aggregates. When onion-like aggregates appear as lamellar mesophase emulsified droplets, the contact with their suspension to the crystals of water-insoluble dyes will solubilize Sudan III molecules at the outer bilayers of the aggregates, while the diffusion to the interior of the aggregates will be slow. Notice that Sudan III molecules are relatively large and their diffusion in the very viscous medium formed by the bilayers, and through the aqueous layer between bilayers, will be very slow. Figure 4 shows that there is a small slope that

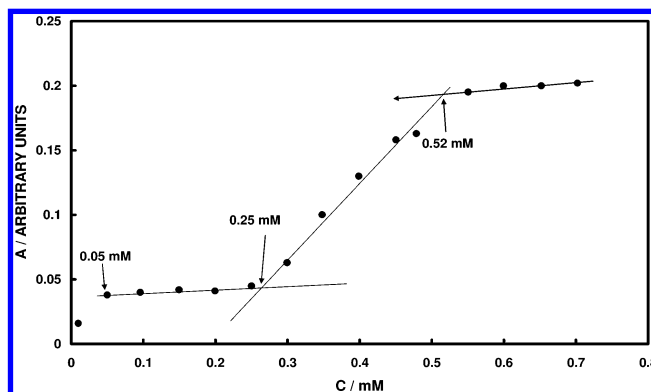


**Figure 4.** Absorbance of solubilized Sudan III in DPA aqueous solutions at  $\lambda = 488$  nm. The lines represent the absorbance profile at different concentration regions separated by the critical points.

reflects the increase in the concentration (or size) of the outer bilayers of aggregates with the total concentration.

The specific conductivity ( $\kappa$ ) of DPA aqueous solutions is represented as a function of the concentration in Figure 5. Two different transition points can be seen, at 0.39 and 0.60 mM. The conductivity profile is rather unusual when compared to those obtained for common ionic surfactants near the cmc. Since  $\kappa$  is the conductivity per unit volume of the system, a decrease with increasing concentration may appear when the system includes liquid crystals, because part of the volume is occupied by nonconductive material. Another decrease may be caused by the capture of counterions by the aggregates. Since counterions are the highly conductive  $H^+$  ones, this may affect considerably the specific conductivity. The reduction of the operative  $K_a$  values with increasing concentration (see below) indicates that this is probably the cause for the slight decrease in  $\kappa$ .

Several representations are useful to highlight different features of  $\kappa$ . For instance,  $\Delta\kappa$  ( $=\kappa_{\text{exp}} - \kappa_{\text{extrapolated}}$ ) where  $\kappa_{\text{exp}}$

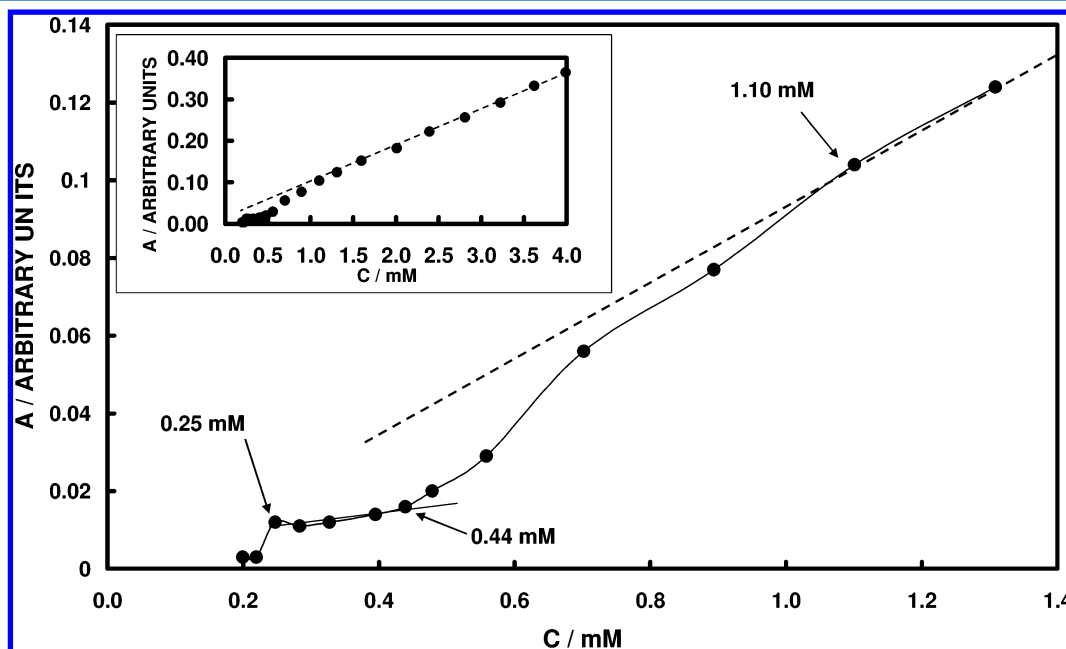


**Figure 3.** Absorbance of diluted DPA aqueous solutions at  $\lambda = 450$  nm. Inset: The complete plot including more concentrated DPA solutions. The solid line is a guide to the eyes, while the dashed line represents the extrapolation of the absorbance at high concentrations.

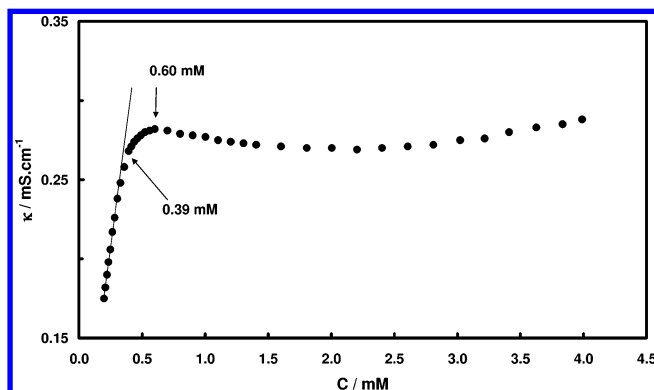


**Figure 5.** Specific conductivity of DPA aqueous solutions as a function of the surfactant concentration. The line represents the extrapolation of  $\kappa$  at low concentrations.

is the experimental  $\kappa$  and  $\kappa_{\text{extrapolated}}$  is the value of  $\kappa$  extrapolated from the very low concentration data) magnifies the slope changes of  $\kappa$  as a function of the surfactant concentration (Figure 2 in the Supporting Information). Three transition points are observed from this representation at 0.30, 0.35, and 0.414 mM. The meaning of the different transition concentrations will be determined later in conjunction with the results of the other techniques. The differential conductivity  $\partial\kappa/\partial C$  also exhibits changes at the concentrations 0.376, 0.40, 0.65, and 1.43 mM (see Figure 6).

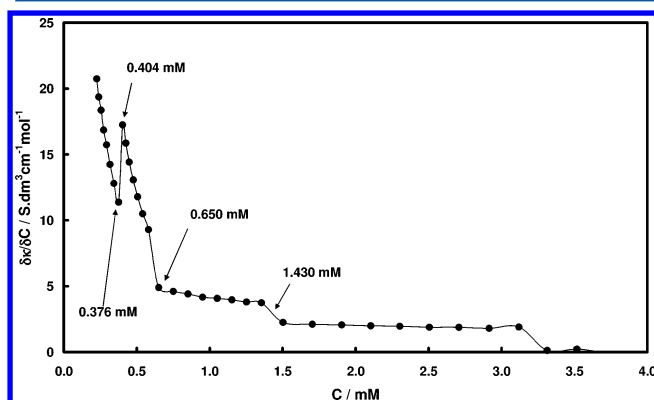


**Figure 6.** Differential conductivity of DPA aqueous solutions as a function of the concentration.

The first part of this plot (below 0.376 mM) indicates that probably small pre-micelles are formed. The minimum indicates the formation of micelles, initially highly ionized which causes the maximum at 0.404 mM. When the size of micelles increases with concentration, they capture counterions and the conductivity decreases. This is mainly due to the high conductivity of counterions ( $\text{H}^+$ ), since the contribution of micelles themselves is lower.<sup>27</sup> The plateau starting at 0.65 mM indicates the formation of larger aggregates whose contribution to the increase of conductivity is small, and the step at 1.43 mM indicates the formation of aggregates having still less conductivity. This indicates that the charge carrier concentration augments parallel to the total surfactant concentration increase, but their individual contribution to conductivity remains constant; i.e., their structure in the concentration range of the step remains unchanged. At about 3.3 mM, the differential conductivity falls to zero, which indicates that almost all the added surfactant goes to the interior of scarcely

conductive aggregates, such as liquid crystalline lamellae, probably onion-like aggregates in the mesophase emulsion. Only the surfactant molecules at the surface of these aggregates contribute to the conductivity. A similar behavior in the system didodecyldimethylammonium bromide–water was interpreted as the transition from very small micelles to small monolayer vesicles, which in turn become larger multilayer vesicles and finally lamellar liquid crystal.<sup>28</sup>

Since the  $\text{p}K_{\text{a}1}$  of DPA is  $3.976 \pm 0.001$ , the surfactant is expected to be negatively charged at  $\text{pH} \sim 7$ . The counterion concentration,  $[\text{H}_3\text{O}^+]$ , as a function of the total DPA concentration was computed from pH measurements (Figure 3 in the Supporting Information). Three different regions were observed in the corresponding  $[\text{H}_3\text{O}^+]$  vs  $[\text{DPA}]$  plot: (i) the counterion concentration increases from 0.115 until 0.145 mM between 0.25 and 0.358 mM; (ii) it remains constant at  $\sim 0.145$  between 0.358 and 0.701 mM; and (iii) it falls down linearly from 0.145 until 0.070 mM between 0.701 and 4.0 mM. The initial increase is caused by the ionization of the added surfactant molecules which are in monomer or small pre-micellar aggregates, while the plateau is consistent with the formation of micelles in equilibrium with a constant concentration of monomers and counterions. This was verified using ion-selective electrodes in micelles of dodecanephosphonic acid.<sup>12</sup> The reduction in  $[\text{H}_3\text{O}^+]$  at higher DPA concentration is caused by the formation of a lamellar mesophase with lower ionization. The reason for the subsequent decrease is that, when the aggregates grow to form multilamellar vesicles or an emulsified lamellar mesophase, much of the added surfactant is enclosed inside the aggregates and cannot contribute to the formation of hydrogen ions. The larger the aggregates, the lower the proportion of DPA molecules at the aggregates' surface is. Since these molecules are the ones that may be ionized, the total concentration of  $\text{H}_3\text{O}^+$  is reduced.

The viscosity of DPA aqueous solutions as a function of the surfactant concentration also exhibits a peculiar behavior (Figure 7). Very dilute solutions ( $<0.2$  mM) have viscosities

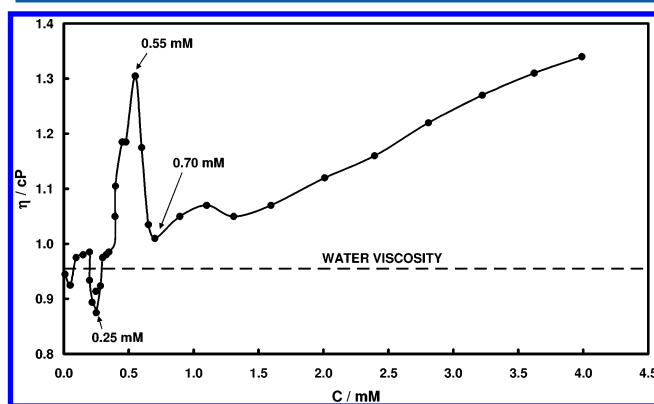


**Figure 7.** Viscosity of DPA aqueous solutions as a function of the total surfactant concentration. The curve is an eye guide.

close to that of pure water. Between 0.2 and 0.3 mM, the viscosity decreases. As reported by several authors in the past,<sup>29,30</sup> this phenomenon might be due to a water-structure-breaking effect by the phosphonic acid groups.<sup>31</sup> Taking into account that the  $\text{p}K_{\text{a}2}$  of *n*-decane phosphonic acid is high ( $=7.985 \pm 0.003$ ),<sup>19</sup> the ionization degree of the phosphonate groups in pure water was computed only with the  $\text{p}K_{\text{a}1}$ ,



**Table 1. Transition Concentrations in Aqueous *n*-Decane Phosphonic Acid Solutions**

<i>a</i> (mol·dm <sup>-3</sup> )	<i>b</i> (mol·dm <sup>-3</sup> )	<i>c</i> (mol·dm <sup>-3</sup> )	<i>d</i> (mol·dm <sup>-3</sup> )	<i>e</i> (mol·dm <sup>-3</sup> )	<i>f</i> (mol·dm <sup>-3</sup> )	method
			0.000394	0.0006		$\kappa$ vs <i>C</i>
	0.0003	0.00035	0.000414			$\Delta\kappa$ vs <i>C</i>
		0.000376	0.000404	0.00065	0.00142	$\partial\kappa/\partial C$ vs <i>C</i>
		0.000358		0.000701		[H <sup>+</sup> ] vs <i>C</i>
0.00005	0.00025	0.0003	0.00044	0.0007	0.0011	<i>A</i> vs <i>C</i>
0.00005	0.00025		0.00052			Sudan III
	0.00025		0.00055	0.0007		$\eta$ vs <i>C</i>
0.00005	0.000260	0.000346	0.000454	0.000670	0.00127	average
	0.000023	0.000033	0.000066	0.000045	0.00023	std. dev.

resulting in  $\alpha \approx 0.059$ , which is the average charge of these groups. The water structure breaking/enhancing ability of ions could be quantified by the change in the average total geometrical factors over all the configurations of a number of water molecules caused by the introduction of a particle of solute ( $\Delta G_{\text{HB}}$ ).<sup>31</sup> Structure enhancers (breakers) cause positive (negative) values of  $\Delta G_{\text{HB}}$ . The  $\Delta G_{\text{HB}}$  value for the almost uncharged phosphonic group was estimated between  $-0.34$  and  $-0.57$ , which corresponds to a strong water structure breaker.<sup>32</sup>

The viscosity increase starting at 0.25 mM might be explained as the formation of disk-like micelles (see below), which are expected to cause perturbation of the solution flux lines due to their geometry. The sudden decrease in viscosity above 0.55 mM might be caused by a destabilization of the disk-like micelles to form vesicles or droplets of lamellar mesophase (Figure 1), i.e., nearly compartmentalized spherical particles whose influence on viscosity is lower than that of asymmetrical particles. This transition occurs between 0.55 and 0.70 mM. Above this latter concentration, a slow viscosity increase obeys its dependence on the volume fraction of the suspended particles.

The wrong cmc value reported in the literature (1.66 mM<sup>14</sup> vs  $0.346 \pm 0.033$  mM found in the present work) could be due to a misinterpretation of conductivity results. This emphasizes the need of employing a battery of techniques to determine the cmc of novel surfactants. A precedent of a similar misinterpretation based on single technique measurements occurred with alkyltrimethylammonium hydroxides.<sup>33</sup>

The transition concentration values observed from the battery of experimental techniques employed in the present work are summarized in Table 1. The average values of these concentrations together with the expected associated processes are: (a) the formation of premicelles with some capacity to solubilize dyes (0.05 mM); (b) formation of spherical micelles which immediately grow to form disk-like micelles ( $0.260 \pm 0.023$  mM); (c) undetermined structure transition of the disk-like micelles ( $0.346 \pm 0.033$  mM); (d) destabilization of the disk-like micelles ( $0.454 \pm 0.066$  mM); (e) formation of the lamellar mesophase emulsion ( $0.670 \pm 0.045$  mM); and (c) undetermined transition ( $0.127 \pm 0.023$  mM).

It is noteworthy that, in a research on polyethylene glycol (PEG) decorated lipid bilayer by cryo-transmission electron microscopy and dynamic light scattering, the same sequence of structures was found. By dilution of a disperse lamellar phase, first small discoidal micelles form which coexist with liposomes, and by further dilution, the disk-like micelles become spherical ones.<sup>34</sup>

**Molecular Dynamics Simulations.** As described in the Experimental Section, different numbers of DPA molecules at random positions and orientations were introduced in SPC water boxes. In all cases, the surfactants spontaneously self-aggregated in the ns time scale (Figure 8), forming structures whose geometry depends on the local concentration (see below).

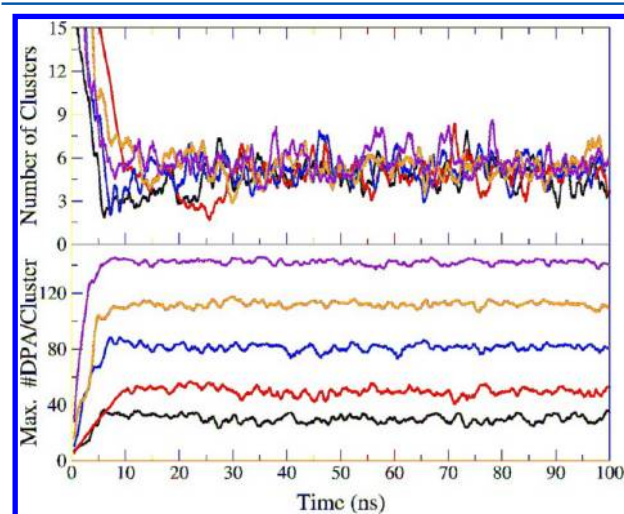


**Figure 8.** Number of clusters in the simulation box (top) and maximum number of molecules per cluster (bottom) as a function of time for the trajectories with 40 (black), 60 (red), 90 (blue), 120 (orange), and 150 (violet) DPA molecules.

As expected, the number of clusters decreases while their size grows as a function of time. A premicellar state is reached at about 10 ns. Irrespective of the number of DPA molecules in the simulation box, approximately five surfactant molecules stay apart from the main aggregate, as free monomers (Figure 7). The same behavior, corresponding to equilibrium between the aggregates and free species, has been previously reported for *n*-dodecane phosphonic acid micelles and lamellar liquid crystal performed with ion-selective electrodes.<sup>12</sup>

The shape evolution of the aggregates can be described by their principal moments of inertia (Figure 4 in the Supporting Information). Small, nearly spherical aggregates have similar moments of inertia along the three principal axes. For disk-like micelles, the moment of inertia with respect to the symmetry axis of the disk is significantly different, while the other two are more similar. Our results show that aggregates formed by 90 or less DPA molecules are almost spherical, while those corresponding to larger aggregates are asymmetric (Figure 9).

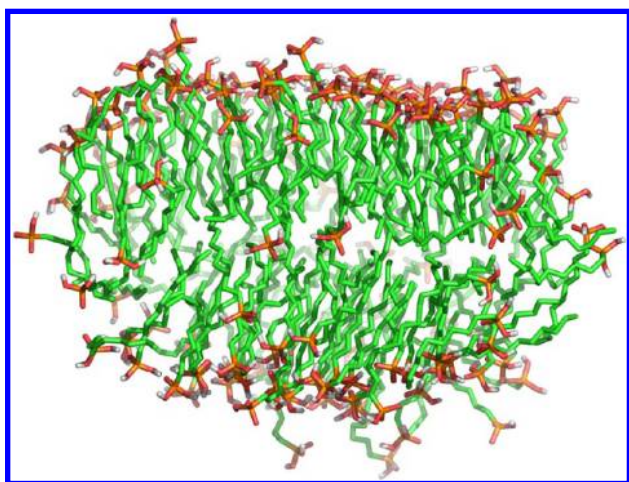


**Figure 9.** Snapshot corresponding to the lateral cross section of a disk-like micelle consisting of 150 DPA molecules obtained after 100 ns of MD simulation.

The solvent accessible surface (SAS) per molecule in the aggregates also exhibits a large dependence on time, becoming constant after  $\sim 10$  ns (Figure 10), in agreement with the results

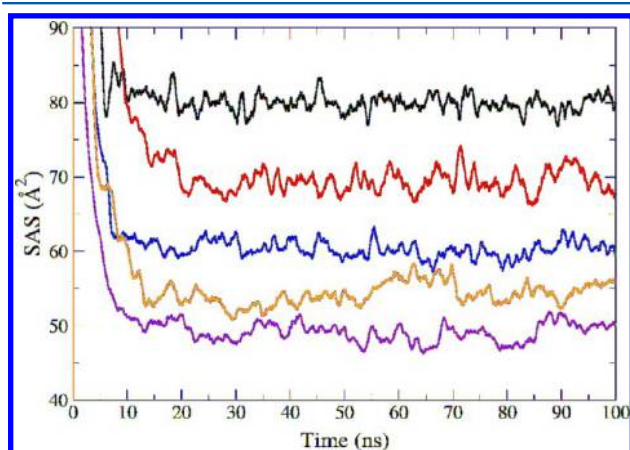


**Figure 10.** Solvent accessible surface (SAS) per molecule in the aggregates as a function of time for the trajectories with 40 (black), 60 (red), 90 (blue), 120 (orange), and 150 (violet) DPA molecules.

shown in Figure 8 above and in Figure 5 of the Supporting Information. Moreover, this property is highly sensitive to the number of surfactant molecules in the micelles, decreasing for increasing number of micellized surfactants. In a recent study on lysophospholipid micelles, Brocos et al.<sup>35</sup> reported an empirical linear correlation between the SAS area per surfactant and the ratio  $n/n_s$ , where  $n_s$  stands for the number of micellized molecules and  $n$  is the number of carbon atoms in the surfactant tail group. This relation is not strictly linear for DPA aggregates (Figure 5 in the Supporting Information), its slope slowly decreasing with  $n/n_s$ . This encourages us to predict an asymptotic SAS value at about  $0.5 \text{ nm}^2$ , corresponding to more than 150 DPA molecules, at which a lamellar mesophase is expected to be formed.

As it can be seen, aggregates having 40–60 DPA molecules show a significantly higher SAS value than those having  $n_s \geq 90$ . This is consistent with changes in micelle shape when increasing the aggregation number. The areas occupied by a phosphonic acid group in DPA anhydrous crystals are  $27.8 \pm 1.3 \text{ \AA}^2$ ,<sup>36</sup> while that occupied by a dodecane phosphonic acid molecule at the air–water interface below the cmc is  $99.53 \pm 0.01 \text{ \AA}^2$ . This was attributed to a liquid expanded state.<sup>15</sup> The excluded area per phosphonic acid headgroup computed from the polar headgroup partial molar volume in micellized state is  $35 \pm 13 \text{ \AA}^2$ .<sup>15</sup> This latter value may be taken as the hydrophilic SAS. The average SAS value obtained for the micelles with 150 DPA molecules (between 10 and 100 ns) is  $49 \pm 2 \text{ \AA}^2$ , which is in between the crystallographic and adsorbed areas. Using the excluded area,  $15 \text{ \AA}^2$  per surfactant molecule is exposed to water as the hydrophobic SAS, i.e., 30% of the total SAS. This percentage is similar to that presented by several lysophospholipids (between 27 and 41%).<sup>35</sup> Considering the area occupied by a water molecule in liquid state as  $10.5 \text{ \AA}^2$  (estimated from bulk-density data) or  $8.1 \text{ \AA}^2$  for nonassociated molecules,<sup>37</sup> between 1.4 and 1.9 water molecules per DPA molecule, on average, can be estimated. It is worth mentioning that most of the SAS in the largest aggregates comes from interactions along the perimeter of the disk-shaped micelles (Figure 9) which, as explained above, is difficult to stabilize.

The interaction between the surfactant polar heads seems to be the key for the formation of disk-like micelles. The

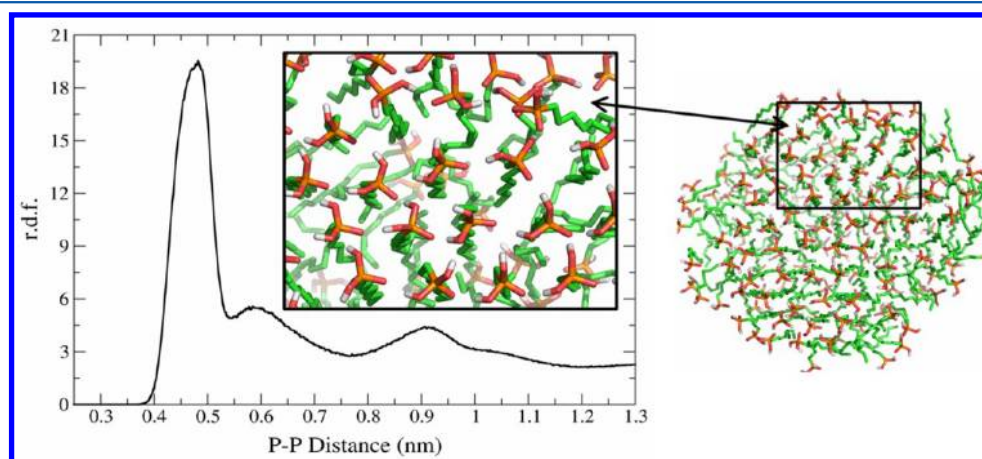


**Figure 11.** Phosphorus–phosphorus radial distribution function obtained for the aggregate with 150 DPA molecules after 100 ns of simulation time (left) together with a snapshot of the corresponding structure (right) and a magnification highlighting the relative position and orientation of the surfactant heads (inset).



characteristic distance between neighbor P atoms (5.3 Å) is revealed by the radial distribution function (rdf) (Figure 11).

As seen in Figure 11 (inset), the surfactant heads are interconnected by a network of H-bonds. The mean lifetime ( $\tau$ ) of these interactions can be approached as the time at which the normalized decay function ( $N/N_0$ ), with  $N$  being the number of contacts that remain after a given time and  $N_0$  the initial number of contacts, equals  $e^{-1}$ <sup>38,39</sup> (see Figure 12). The

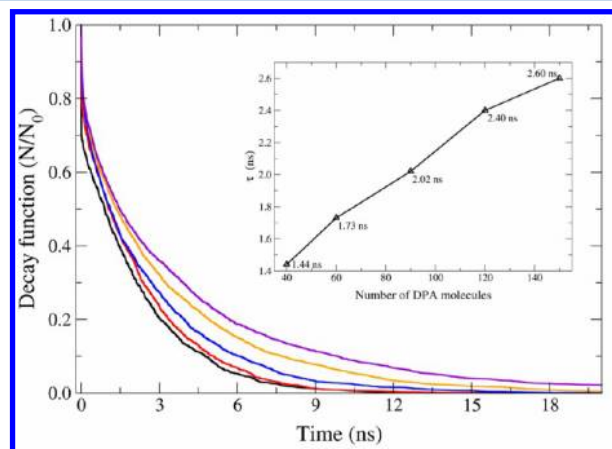


**Figure 12.** Decay function for the head–head surfactant interactions as a function time for the trajectories with 40 (black), 60 (red), 90 (blue), 120 (orange), and 150 (violet) DPA molecules. The mean lifetime obtained from the decay function is also represented (inset) as a function of the number of surfactants in the aggregates (the line is just a guide to the eyes).

cutoff distance considered to define the head–head contacts is 5.3 Å between the corresponding P atoms, matching the distance at the first peak of the rdf shown in Figure 11. The analysis performed over the five trajectories shows that  $\tau$  increases almost linearly for increasing aggregation number of the micelle, ranging from 1.44 ns for 40 micellized DPA to 2.60 ns for 150 aggregated surfactants (Figure 12, inset). Therefore, the larger the micelle, the more stable the interactions between surfactants are.

The mean lifetimes obtained for the head–head surfactant interactions (Figure 12, inset) are about 4 orders of magnitude larger than those of liquid water.<sup>40–44</sup> In decyltrimethylammonium bromide micelles, the exchange of monomers between the micelle and bulk water was estimated to occur in the time scale of 10–100 ns.<sup>45</sup> Similar rates are expected for the exchange of DPA molecules between aggregates and the intermicellar solution. Studies of the relaxation time of water, which may be interpreted as the lifetime of a water cluster, gave values between 0.9<sup>43</sup> and 8 ps.<sup>42</sup> Then, the responsibility of the strong hydrogen bond between the surfactant headgroups in micelles is probably a combination of the crowding of the surfactant molecules in aggregates (see Figure 11), the restrictions in their lateral movement in the Stern layer, and the higher permanency of surfactant molecules in aggregates when compared with that of water molecules in bulk clusters. These factors reduce the thermal perturbations that originate the exchange of H-bonds between different molecules. Also, this strong intermolecular H-bond network may be the reason why DPA crystals are anhydrous (no hydration water molecules have been detected by DSC measurements<sup>11</sup>).

Each DPA molecule may form up to five H-bonds, including those with water and other surfactant molecules (Figure 13).

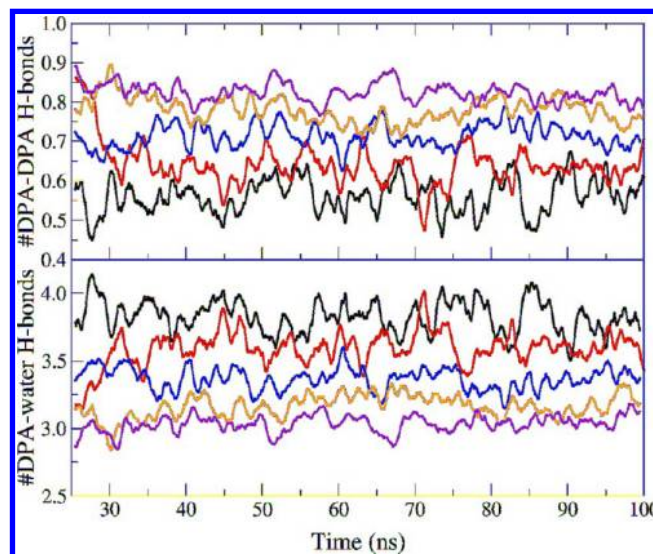


**Figure 13.** Number of surfactant–surfactant (top) and surfactant–water (bottom) hydrogen bonds per molecule as a function of time for the trajectories with 40 (black), 60 (red), 90 (blue), 120 (orange), and 150 (violet) DPA molecules. The H-bond definition was based on a geometrical criterion with a distance cutoff of 0.35 nm and an angle cutoff of 30°.

The number of surfactant–surfactant H-bonds increases with the number of DPA molecules in the micelle. However, the number of surfactant–water H-bonds shows the opposite trend (Figure 13), as expected for a transformation from spherical to disk-like aggregates. In spherical aggregates, the surface density of  $-\text{PO}_3\text{H}_2$  groups and thus the occurrence of headgroup–headgroup interactions is moderate, while the interaction between headgroups and water molecules is more likely. The transformation to lamellar aggregates increases the close packing of the phosphonic acid groups in the planar surfaces as well as the number of headgroup–headgroup H-bonds, to the detriment of DPA–water contacts. Upon the formation of disk-like micelles, the interactions between acid groups increase in the flat region, even as those in the edges of the disk remain comparable to those in spherical micelles. Since the ratio of molecules in the edges to those in the planar surfaces decreases as the size of the disk-like structure increases, the average number of H-bonds also keeps the same trend. For instance, Figure 13 shows the number of H-bonds in aggregates with 120 and 150 DPA molecules is much closer than that between structures with a lower number of surfactants. Previous works stated that in alkane phosphonic acid aggregates (micelles and lamellar liquid crystals) there is a significant H-bond interaction among the acid groups,<sup>11,46–48</sup> which is confirmed by the present results. A reduction in the amount of water molecules close to the polar headgroups is expected to lower the ionization equilibrium of the phosphonic acid groups, due to the mass-action rule. This would produce a drop in the apparent acidity constant ( $K_{a1}$ ) and an increase of  $\text{p}K_{a1}$  when the size of the aggregates grows. This has already been observed in aqueous *n*-dodecanephosphonic acid systems,<sup>12</sup> where the  $\text{p}K_{a1}$  varies from 4.03 in non-micellized molecules to about 6 in micelles and 6.74 in lamellar mesophases. Moreover, the approaching between polar head groups produces an increase in the Stern layer surface potential, which in turn causes a reduction in the micelle ionization degree. Since the counterions are  $\text{H}_3\text{O}^+$  ions, this also leads to a reduction in the effective

ionization constant of the phosphonic acid groups in aggregates.

The radial distribution function of the water oxygen atoms with respect to the phosphorus, the first and second carbon atoms of the DPA molecules show that the water molecules do not penetrate the micelle structures, only the surfactant head and the first carbon atom being in contact with the solvent molecules (Figure 14). In general, it is accepted that the first

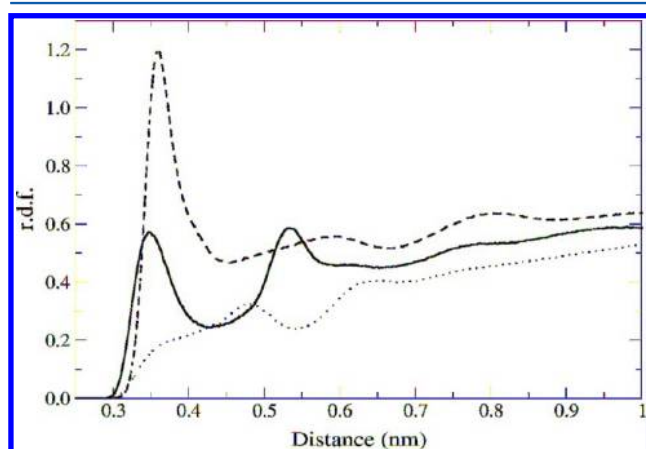


**Figure 14.** Radial distribution function of water oxygen atoms with respect to the phosphorus of the headgroup (dashed line) and the first (solid line) and second (dotted line) carbon atoms of DPA for the system with 150 surfactant molecules.

two or three methylene groups near the polar headgroup can be in contact with water in spherical micelles. Because of the dense packing of the phosphonic acid groups in the DPA micelles, the “wetting” of only the  $\alpha$ -methylene group seems to be reasonable, as it has also been deduced above from the SAS values.

## DISCUSSION

As stated above, disk-like micelles are less common than spherical or rod-like aggregates. This could be explained by the difficulty to stabilize the perimeter of such structures due to its line tension. This often causes the growth of the aggregate, giving rise to the formation of large bilayers which may fold to form vesicles.<sup>1</sup> Inverse disk-like micelles have been proposed as an interpretation of X-ray diffraction patterns of some liquid crystals formed by heating anhydrous or quasi-anhydrous surfactants. They have been found in a number of potassium,<sup>49</sup> rubidium,<sup>50</sup> strontium,<sup>51</sup> and sodium<sup>52,53</sup> soaps. The aggregation number of such disk-like structures depends on the temperature. As an example, in potassium tetradecanoate, it ranges from 210 (between 195 and 218 °C) to 74 (between 244 and 270 °C).<sup>49</sup> Normal disk-like micelles were informed in aqueous medium for sodium dodecyl sulfate (SDS) in the presence of several cosolutes.<sup>54–56</sup> The size of those micelles depends on the specific medium composition (electrolytes or alcohols), and the diameter is reduced with increasing water content. The addition of the hydrophobic counterion *p*-toluidine hydrochloride to SDS also causes the transformation of rod-like to disk-like micelles.<sup>40</sup> The system formed by SDS, cocamidopropyl betaine, and dodecanoic acid produces disk-like micelles as well.<sup>57</sup> The two latter systems may form nematic discotic mesophases at high concentration. Phospholipid disk-like micelles are predicted from energetic consid-

erations as intermediates in the formation of vesicles.<sup>7–9</sup> The formation of such structures was described in literature studying bile salt/lecithin micelles.<sup>10,58</sup>

A mechanism to form vesicles by detergent depletion uses mixed micelles of uncharged phospholipids and surfactants.<sup>2–5</sup> Disk-like micelles are formed as halfway structures, which then are transformed into vesicles by removing the conventional surfactant. The discoidal micelles are stabilized by the accumulation of surfactant molecules in the edges of the structures. The elimination of these molecules causes destabilization by exposition of the phospholipid hydrophobic groups to the solvent. This, in turn, induces the growth of the micelles which become large bilayers and subsequently seal off their exposed hydrophobic edges to form vesicles. A generalization of this model postulates that discoidal micelles can be formed in some cases without the presence of a second amphiphile, as short-lived “flakes” or fragments of bilayers.<sup>18</sup> These later structures could also form vesicles upon sonication or when they are forced to pass through a narrow filter.

Considering the schemes proposed for other systems as well as the information collected in the present work, the disk-like micelles elucidated for DPA are proposed as intermediate structures in the vesicle formation pathway. Since this surfactant is a rather weak acid ( $pK_{a1} = 3.976 \pm 0.001$ ,  $pK_{a2} = 7.985 \pm 0.003$ ),<sup>19</sup> the polar groups of some of the dissolved molecules are ionized to  $-\text{PO}_3\text{H}^-$ , as can be seen in Figure 3 of the Supporting Information from very dilute solutions up to about 0.36 mM. The ionized molecules act as standard anionic surfactants, and they are expected to migrate to the edges of discoid micelles formed by uncharged molecules. The curvature at the edges is compatible with ionic amphiphiles. This could favor the stabilization of such structures. Besides, micellization reduces the ionization constant of the acid. On the basis of measurements on the *n*-dodecane phosphonic acid (DoPA)–water system,<sup>12</sup> the value of  $pK_{a1}$  (first acid ionization) for micellized DPA must be  $pK_{a1,\text{mic}} \approx 5.83$ . This means that the proportion of ionized to un-ionized molecules is reduced and the size of disk-like micelles is expected to increase until they become unstable and form bilayers, or start to bend and form vesicles. This may occur in the short concentration range in which  $[\text{H}_3\text{O}^+]$  remains constant, between 0.36 and 0.70 mM (Figure 3 in the Supporting Information). Also, by extrapolation from data of the DoPA–water system,<sup>12</sup> the value of  $pK_{a1}$  in the domain of the concentrated lamellar mesophase of DPA must be  $pK_{a1,\text{LM}} \approx 6.1$ . This may cause the reduction in  $[\text{H}_3\text{O}^+]$  in the explored concentration range above 0.70 mM (Figure 3 in the Supporting Information). Since the transitions are gradual, the apparent  $pK_{a1}$  values, which are an average of those of monomers and aggregates of different size and nature, will increase with concentration (Figure 15). Three different linear regimes of variation of  $pK_{a1}$  with  $\log C$  may be observed: (i) the low concentration regime ends at 0.33 mM ( $pK_{a1} = (0.81 \pm 0.11) \log C + 4.370 \pm 0.067$ ;  $r^2 = 0.9790$ ); (ii) a second region exists between 0.33 and 1.3 mM ( $pK_{a1} = (1.475 \pm 0.030) \log C + 4.6745 \pm 0.0082$ ;  $r^2 = 0.9981$ ); and (iii) above 1.3 mM ( $pK_{a1} = (2.198 \pm 0.051) \log C + 4.598 \pm 0.022$ ;  $r^2 = 0.9985$ ). All error intervals were computed with a confidence level of 0.90. It is evident from a statistical point of view that the three straight lines are different.

## CONCLUDING REMARKS

Our experimental results indicate that the cmc reported in the literature is too high and probably arises from a misinter-



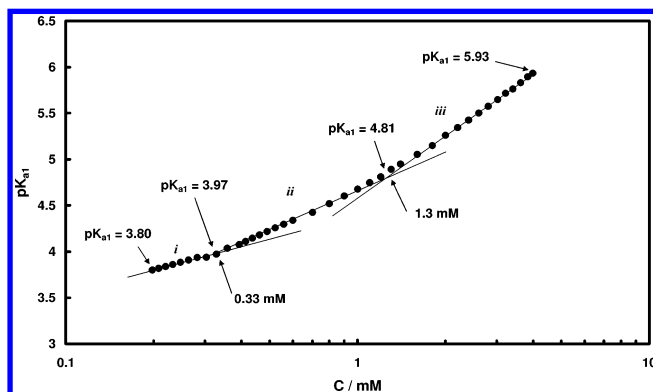


**Figure 15.** Apparent  $pK_{a1}$  values for diluted DPA aqueous solutions. Lines are least-squares fits.

pretation of the specific conductivity vs concentration plot. This emphasizes the need to verify with different techniques the interpretation of the critical points when new surfactants are studied. The aggregation pathway of DPA is as follows: (i) at 0.05 mM, premicelles with some capacity to solubilize dyes are formed; (ii) at  $0.260 \pm 0.023$  mM, probably spherical micelles are formed, which immediately grow to asymmetrical structures; (iii) at  $0.454 \pm 0.066$  mM, the disk-like micelles become unstable, giving rise to the formation of an emulsion of lamellar mesophase; and (iv) at  $0.670 \pm 0.045$  mM, the system is formed only by a lamellar mesophase emulsion. The structure of different micelles, including discoid aggregates, is described in detail by MD simulations. The formation of a strong network of intermolecular H-bonds among the surfactant headgroups produces a compact polar layer with low water content. Such H-bond network seems to be responsible for the stable disk-like micelles observed at high local concentration. The density of DPA–DPA contacts decreases with decreasing aggregation number, while the interaction between the surfactant molecules and water becomes more important. The simulations also predict that the concentration of non-micellized DPA molecules remains constant with increasing concentration above the cmc, as expected in equilibrated systems. Experimental and computational results match well in the main conclusions on this system. Overall, disk-like micelles claim as intermediate structures for more complex arrangements such as vesicles and lamellar mesophases.

## ■ ASSOCIATED CONTENT

### ● Supporting Information

Figures showing a photomicrograph of the 15.78 mM DPA suspension in water, amplification of the very low concentration zone of  $\kappa = \kappa_{\text{measured}} - \kappa_{\text{extrapolated}}$  vs  $C$  of aqueous solutions of DPA, concentration of hydrogen ions as a function of the total DPA concentration in water, principal moments of inertia of the DPA aggregates as a function of time, and dependence of SAS on  $n/n_s$  for DPA aggregates. This material is available free of charge via the Internet at <http://pubs.acs.org>.

## ■ AUTHOR INFORMATION

### Notes

The authors declare no competing financial interest.

## ■ ACKNOWLEDGMENTS

This work was supported by a grant from the MINECO-Spain (MAT2011-25501). E.P.S. is an assistant researcher of the

Consejo Nacional de Investigaciones Científicas y Técnicas de la República Argentina (CONICET) and acknowledges CONICET for a fellowship which enabled her to travel to the University of Santiago de Compostela (Spain) to do this research. Á.P. is an Isidro Parga Pondal fellow (Xunta de Galicia). The experimental part was supported by a grant of the Universidad Nacional del Sur (Argentina). We are grateful to the “Centro de Supercomputación de Galicia” (CESGA) for computing time.

## ■ REFERENCES

- (1) Gradzielski, M. The Rheology of Vesicle and Disk Systems—Relations between Macroscopic Behaviour and Microstructure. *Curr. Opin. Colloid Interface Sci.* **2011**, *16*, 13–17.
- (2) Lasic, D. D. A Molecular Model for Vesicle Formation. *Biochim. Biophys. Acta* **1982**, *692*, 501–502.
- (3) Cornell, M. A.; Middlehurst, J.; Separovic, F. Small Unilamellar Phospholipid Vesicles and the Theories of Membrane Formation. *Faraday Discuss. Chem. Soc.* **1986**, *81*, 163–178.
- (4) Lasic, D. D. A General Model of Vesicle Formation. *J. Theor. Biol.* **1987**, *124*, 35–41.
- (5) Schurtenberger, P.; Mazer, N.; Walvogel, S.; Kanzig, W. Preparation of Monodisperse Vesicles with Variable Size by Dilution of Mixed Micellar Solutions of Bile Salt and Phosphatidylcholine. *Biochim. Biophys. Acta* **1984**, *775*, 111–114.
- (6) Lasic, D. D. The Mechanism of Vesicle Formation. *Biochem. J.* **1988**, *256*, 1–11.
- (7) Fergason, J. L.; Brown, H. G. Liquid Crystals and Living Systems. *J. Am. Oil Chem. Soc.* **1968**, *45*, 120–127.
- (8) Franck, F. C. On the Theory of Liquid Crystals. *Discuss Faraday Soc.* **1958**, *25*, 19–28.
- (9) Helfrich, W. The Size of Bilayer Vesicles Generated by Sonication. *Phys. Lett.* **1974**, *50a*, 115–116.
- (10) Mazer, N. A.; Benedeck, G. B.; Carey, M. C. Quasielastic Light-Scattering of Aqueous Biliary Lipid Systems. Mixed Micelle Formation in Bile Salt-Lecithin Solutions. *Biochemistry* **1980**, *19*, 601–615.
- (11) Schulz, P. C.; Abrameto, M.; Puig, J. E.; Soltero-Martínez, F. A.; González-Alvarez, A. Phase Behavior of the Systems *n*-Decanephosphonic Acid - Water and *n*-Dodecanephosphonic Acid- Water. *Langmuir* **1996**, *12*, 3082–3088.
- (12) Minardi, R. M.; Schulz, P. C.; Vuano, B. The Aggregation of *n*-Dodecanephosphonic Acid in Water. *Colloid Polym. Sci.* **1996**, *274/11*, 1089–1093.
- (13) Lasic, D. D. Mixed Micelles in Drug Delivery. *Nature* **1992**, *355*, 279–280.
- (14) Demchenko, P.; Yaroshenko, N. Temperature Effect on the Critical Micelle Concentration of Aqueous Solutions of Alkanephosphonic Acids and Their Aqueous Solutions (In Russian). *Fiz.-Khim. Mekh. Liofil'nost Dispersnykh Sist.* **1973**, *4*, 91–95.
- (15) Schulz, P. C.; Minardi, R. M.; Gschaidner de Ferreira, M. E.; Vuano, B. The Interface Air/Water of *n*-Dodecanephosphonic Acid Solutions. *Colloid Polym. Sci.* **1998**, *276*, 52–58.
- (16) Schulz, P. C. Steric Fitting of the Rodlike Micelle Size. *J. Colloid Interface Sci.* **1992**, *152* (2), 333–337.
- (17) Gruen, D. W. A Model for the Chains in Amphiphilic Aggregates. Comparison with a Molecular Dynamics Simulation of a Bilayer. *J. Phys. Chem.* **1985**, *89*, 146–153.
- (18) Israelachvili, J. N.; Mitchell, D. J.; Ninham, B. W. Theory of Self-Assembly of Hydrocarbon Amphiphiles into Micelles and Bilayers. *J. Chem. Soc., Faraday Trans.* **1976**, *2* (72), 1525–1568.
- (19) Schulz, P. C.; Lelong, A. L. M. Ionization Constants of *n*-Decane Phosphonic Acid (In Spanish). *Rev. Latinoam. Quím.* **1976**, *7*, 9–16.
- (20) Oostenbrink, C.; Villa, A.; Mark, A. E.; van Gunsteren, W. F. A Biomolecular Force Field Based on the Free Enthalpy of Hydration and Solvation: The GROMOS Force-Field Parameter Sets 53A5 and 53A6. *J. Comput. Chem.* **2004**, *25*, 1656–1676.

- (21) Roy, S.; Ataol, T. M.; Muller-Plathe, C. Molecular Dynamics Simulation of Heptyl Phosphonic Acid: A Potential Component for Fuel Cell Polymer Membrane. *J. Phys. Chem. B* **2008**, *112*, 7403–7409.
- (22) Malde, A. K.; Zuo, L.; Breeze, M.; Stroet, M.; Poger, D.; Nair, P. C.; Oostenbrink, C.; Mark, A. E. An Automated Force Field Topology Builder (ATB) and Repository: Version 1.0. *J. Chem. Theory Comput.* **2011**, *7* (12), 4026–4037.
- (23) Berendsen, H. J. C.; Van de Spoel, D.; van Drunen, R. Gromacs: A Message-Passing Parallel Molecular Dynamics Implementation. *Comput. Phys. Commun.* **1995**, *91*, 43–56.
- (24) Lindahl, E.; Hess, B.; van der Spoel, D. GROMACS 3.0: A Package for Molecular Simulation and Trajectory Analysis. *J. Mol. Model.* **2001**, *7*, 306–317.
- (25) van der Spoel, D.; Lindahl, E.; Hess, B.; Groenhof, G.; Mark, A. E.; Berendsen, H. J. C. GROMACS: Fast, Flexible and Free. *J. Comput. Chem.* **2005**, *26*, 1701–1718.
- (26) LeBard, D. N.; Levine, B. G.; DeVane, R.; Shinoda, W.; Klein, M. L. Premicelles and Monomer Exchange in Aqueous Surfactant Solutions above and below the Critical Micelle Concentration. *Chem. Phys. Lett.* **2012**, *522*, 38–42.
- (27) Schulz, P. C.; Hernández-Vargas, M. E.; Puig, J. E. Do Micelles Contribute to the Total Conductivity of Ionic Micellar Systems? *Lat. Am. Appl. Res.* **1995**, *25*, 153–159.
- (28) Soltero, J. F. A.; Bautista, F.; Pecina, E.; Puig, J. E.; Manero, O.; Proverbio, Z.; Schulz, P. C. Rheological Behavior in the Didodecyldimethylammonium Bromide/Water System. *Colloid Polym. Sci.* **2000**, *278*, 37–47.
- (29) Schwenk, C. F.; Hofer, T. S.; Rode, B. M. “Structure Breaking” Effect of Hydrated Cs<sup>+</sup>. *J. Phys. Chem. A* **2004**, 1509–1514.
- (30) Mancinelli, R.; Botti, A.; Bruni, M. A.; Soper, B. A. K. Perturbation of Water Structure due to Monovalent Ions in Solution. *Phys. Chem. Chem. Phys.* **2007**, *9*, 2959–2967.
- (31) Marcus, Y. Effect of Ions on the Structure of Water: Structure Making and Breaking. *Chem. Rev.* **2009**, *109*, 1346–1370.
- (32) Rodríguez, J. L.; Minardi, R. M.; Ciolino, A.; Pieroni, O.; Vuano, B.; Schulz, E. P.; Schulz, P. C. Effect of an Amphiphilic Polymer on the Evaporation Behavior of its Solutions in Toluene and in Water. *Colloids Surf., A* **2009**, *352*, 74–78.
- (33) Schulz, P. C.; Morini, M. A.; Minardi, R. M.; Puig, J. E. The Aggregation in Dodecyltrimethylammonium Hydroxide Aqueous Solutions. *Colloid Polym. Sci.* **1995**, *273* (10), 959–966.
- (34) Johnsson, M.; Edwards, K. Liposomes, Disks, and Spherical Micelles: Aggregate Structure in Mixtures of Gel Phase Phosphatidylcholines and Poly(ethylene glycol) Phospholipids. *Biophys. J.* **2003**, *85*, 3839–3847.
- (35) Brocos, P.; Mendoza-Espinosa, P.; Castillo, R.; Mas-Oliva, J.; Piñeiro, A. Multiscale Molecular Dynamics Simulations of Micelles: Coarse Grain for Self-Assembly and Atomic Resolution for Finer Details. *Soft Matter* **2012**, *8*, 9005–9014.
- (36) Schulz, P. C. Crystalline Structure of n-Decane and n-Dodecane Phosphonic Acids and Their Mono- and Disodic Salts (in Spanish). *An. Asoc. Quim. Argent.* **1983**, *71*, 271–286.
- (37) Müller, E. A.; Rull, L. F.; Vega, L. F.; Gubbins, K. E. Adsorption of Water on Activated Carbons: a Molecular Simulation Study. *J. Phys. Chem.* **1996**, *100*, 1189–1196.
- (38) Jardón-Valadez, E.; Bondar, A. N.; Tobias, D. J. Dynamics of Internal Water Molecules in Squid Rhodopsin. *Biophys. J.* **2009**, *96*, 2572–2576.
- (39) Piñeiro, Á.; Bond, P. J.; Khalid, S. Exploring the Conformational Dynamics and Membrane Interactions of PorB from *C. glutamicum*: A Multi-Scale Molecular Dynamics Simulation Study. *Biochim. Biophys. Acta, Biomembr.* **2011**, *1808* (6), 1746–1752.
- (40) Rey, R.; Maller, K. B.; Hynes, J. T. Hydrogen Bond Dynamics in Water and Ultrafast Infrared Spectroscopy. *J. Phys. Chem. A* **2002**, *106* (50), 11994–11996.
- (41) Luzar, A. Resolving the Hydrogen Bond Dynamics Conundrum. *J. Chem. Phys.* **2000**, *113*, 10663.
- (42) Tamai, Y.; Tanaka, H.; Nakanishi, K. Molecular Dynamics Study of Polymer-Water Interaction in Hydrogels 2. Hydrogen-Bond Dynamics. *Macromolecules* **1996**, *29*, 6761–6769.
- (43) Yeremenko, S.; Pshenichnikov, M. S.; Wiersma, D. A. Hydrogen-Bonds Dynamics in Water Explored by Heterodyne-Detected Photon Echo. *Chem. Phys. Lett.* **2003**, *369*, 107–113.
- (44) Fecko, C. J.; Eaves, J. D.; Loper, J. J.; Tokmakoff, A.; Geissler, P. L. Ultrafast Hydrogen-Bond Dynamics in the Infrared Spectroscopy of Water. *Science* **2003**, *301*, 1698–1701.
- (45) Pal, S.; Bagchi, B.; Balasubramanian, S. Hydration Layer of a Cationic Micelle, C<sub>10</sub>TAB: Structure, Rigidity, Slow Reorientation, Hydrogen Bond Lifetime and Solvation Dynamics. *J. Phys. Chem. B* **2005**, *109*, 12879–12890.
- (46) Klose, G.; Petrov, A. G.; Volke, F.; Meyer, H. W.; Förster, G.; Rettig, W. Self Assembly and Phase Behaviour of Short Chain Phosphonic Acid-Water Systems in a Wide Concentration Range. Microscopic, NMR and X-ray Diffraction Studies. *Mol. Cryst. Liq. Cryst.* **1982**, *88*, 109–126.
- (47) Schulz, P. C.; Minardi, R. M.; Vuano, B. Solubilization of Styrene in the Catanionic System Dodecyltrimethylammonium Hydroxide - n-Dodecanephosphonic Acid. *Colloid Polym. Sci.* **1998**, *276*, 278–281.
- (48) Minardi, R. M.; Schulz, P. C.; Vuano, B. The Aggregation of Aqueous Dodecylphosphonic Acid - Dodecyltrimethylammonium Hydroxide Mixtures. *Colloid Polym. Sci.* **1996**, *274*, 669–677.
- (49) Vold, M. J.; Macomber, M.; Vold, R. D. True Phases Occurring between True Crystal and True Liquid for Single Anhydrous Soaps. *J. Am. Chem. Soc.* **1941**, *63*, 168–175.
- (50) Vold, R. D. The Phase Rule Behavior of Concentrated Aqueous Systems of a Typical Colloidal Electrolyte: Sodium Oleate. *J. Phys. Chem.* **1939**, *43*, 1213–1231.
- (51) Chapman, D. An Infrared Spectroscopic Examination of Some Anhydrous Sodium Soaps. *J. Chem. Soc.* **1958**, *152*, 784–789.
- (52) Vold, R. D.; Vold, M. J. Thermodynamic Behavior of Liquid Crystalline Solutions of Sodium Palmitate and Sodium Laurate in Water at 90 Degrees. *J. Am. Chem. Soc.* **1939**, *61*, 37–44.
- (53) Luzzatti, V. In *Biological Membranes*; Chapman, D., Ed.; Academic Press: New York, 1968.
- (54) Ekwall, P. In *Advances in Liquid Crystals*; Brown, G. H., Ed.; Academic Press: New York, 1975; Vol. 1.
- (55) Forrest, B. J.; Reeves, L. W. New Lyotropic Liquid Crystals Composed of Finite Nonspherical Micelles. *Chem. Rev.* **1981**, *81* (1), 1–14.
- (56) Amaral, L. Q.; Pimentel, C. A.; Tavares, M. R.; Vanin, J. A Study of a Magnetically Oriented Lyotropic Mesophase. *J. Chem. Phys.* **1979**, *71*, 2940–2945.
- (57) Colafemmina, G.; Recchia, R.; Ferrante, A. S.; Amin, S.; Palazzo, G. Lauric Acid-Induced Formation of a Lyotropic Nematic Phase of Disk-Shaped Micelles. *J. Phys. Chem. B* **2010**, *114*, 7250–7260.
- (58) Small, D. M.; Penkett, S. A.; Chapman, D. Studies on Simple and Mixed Bile Salt Micelles by Nuclear Magnetic Resonance Spectroscopy. *Biochim. Biophys. Acta* **1969**, *176*, 178–189.